NATIONAL ADVISORY COMMITTEE FOR AERONAUTICS

TECHNICAL NOTE 3635

ANALYTICAL STUDY OF MODIFICATIONS TO THE AUTOPILOT OF A FIGHTER AIRPLANE IN ORDER TO REDUCE THE RESPONSE TO SIDE GUSTS

By Charles W. Mathews and James J. Adams

Langley Aeronautical Laboratory
Langley Field, Va.

Washington
March 1956

NATIONAL ADVISORY COMMITTEE FOR AERONAUTICS

TECHNICAL NOTE 3635

ANALYTICAL STUDY OF MODIFICATIONS TO THE AUTOPILOT OF A FIGHTER AIRPLANE IN ORDER TO REDUCE THE RESPONSE TO SIDE GUSTS

By Charles W. Mathews and James J. Adams

SUMMARY

The response to side and rolling gusts of an airplane in combination with several types of autopilots was examined in a previous investigation (NACA TN 3603). The type of autopilot considered in the present investigation, in which heading commands are applied to the aileron channel, was found in the previous investigation to have an undesirably large roll and yaw response to side gusts; however, this type of autopilot was found to have certain salient features providing good turning response to lateral-steering commands.

The present investigation is concerned with a study of the means for reducing the response to side gusts. The results indicate that, through fairly minor modifications to the rudder channel, the response to side gusts can be noticeably reduced. These modifications have no significant effect on the command response.

INTRODUCTION

The usefulness of autopilots in providing airplanes with long-period stability has been recognized for many years. Recently, the use of autopilots to provide precise control under maneuvering conditions has become prevalent; however, the requirement still remains that autopilots provide adequate regulation of disturbances to the airplane such as those which result from atmospheric turbulence. Unfortunately, the autopilot characteristics desirable in one application may detrimentally affect the performance in another. The study reported in reference 1, for example, indicates that an autopilot providing a rapid course response to lateral-steering commands has undesirably large rolling and yawing response to side gusts. Since no extensive study has been made of the gust response of autopilot systems, it was felt that this difficulty might not be basic, but that the gust-response characteristics might be improved without deteriorating the command characteristics. Hence, a simplified theoretical study of this possibility was undertaken.

This study was the basis for the present paper which deals with means for compensating the roll and yaw response to side gusts of a fighter airplane in combination with an autopilot. The autopilot investigated is of the type which applies heading signals to the aileron channel. One flight condition, an altitude of 30,000 feet and a Mach number of 0.7, was studied. Results are presented which compare the response to side gusts of the original and compensating autopilots; the responses to commands are presented also.

SYMBOLS

C_L lift coefficient, $\frac{L}{qS}$

C_l rolling-moment coefficient, $\frac{L'}{qSb}$

C_n yawing-moment coefficient, $\frac{N}{qSb}$

C_Y side-force coefficient, $\frac{Y}{qS}$

b wing span, ft

D nondimensional operator, $\frac{\partial}{\partial t\frac{V}{b}}$

I_{XZ} airplane product of inertia, slug-ft^2

$i = \sqrt{-1}$

K autopilot gain constant

K_X nondimensional radius of gyration about X stability axis, $\frac{k_X}{b}$

K_Z nondimensional radius of gyration about Z stability axis, $\frac{k_Z}{b}$

k_X radius of gyration about X stability axis, ft

k_Z	radius of gyration about Z stability axis, ft
K_{XZ}	nondimensional product of inertia, $\frac{I_{XZ}}{m_b^2}$
L	lift, lb
L'	rolling moment, ft-lb
l_X	ratio of vertical-tail length to wing span
l_Z	ratio of distance between center of pressure of vertical tail and X stability axis to wing span
m	mass of airplane, slugs
N	yawing moment, ft-lb
PSD	power spectral density
p	rolling angular velocity, radians/sec
q	dynamic pressure, $\frac{1}{2}\rho V^2$, lb/sq ft
r	yawing angular velocity, radians/sec
S	wing area, sq ft
s	dimensional operator, $\frac{\partial}{\partial t}$, sec^{-1}
t	time, sec
V	airspeed, ft/sec
Y	side force, lb
β	angle of sideslip, radians
$\bar{\beta}$	output signal from filter of gust-compensating autopilot
δ	control deflection, radians
μ	airplane density ratio, $\frac{m}{\rho S b}$
ρ	air density, slugs/cu ft

σ	angle of sidewash at vertical tail, radians
τ	time constant of filter in gust-compensating system, sec
ϕ	angle of roll, radians
ψ	angle of yaw or heading, radians
ω	circular frequency, radians/sec

Subscripts:

a	aileron
c	command
g	due to gust
o	in still air
r	yawing velocity; r also indicates rudder when referring to deflections δ
t	vertical tail
wb	wing-body combination
β,ϕ,ψ	sideslip, roll, and yaw feedbacks in autopilot loops, respectively

Stability derivatives are denoted symbolically through use of subscript notation. For example:

$$C_{n_\beta} = \frac{\partial C_n}{\partial \beta}$$

$$C_{n_{D^2\phi}} = \frac{\partial C_n}{\partial D^2\phi}$$

$$C_{l_p} = \frac{\partial C_l}{\partial \frac{pb}{2V}}$$

$$C_{n_{\delta_r}} = \frac{\partial C_n}{\partial \delta_r}$$

$$C_{Y_r} = \frac{\partial C_Y}{\partial \frac{rb}{2V}}$$

$$C_{l_{\delta_a}} = \frac{\partial C_l}{\partial \delta_a}$$

DESCRIPTION OF AIRPLANE AND AUTOPILOT

Airplane

The analysis was applied to a jet-propelled fighter airplane with unswept wings. This airplane was chosen because it is currently being employed at the Langley Aeronautical Laboratory in a flight investigation of the basic type of autopilot considered herein. A drawing of the airplane is presented in figure 1, and pertinent dimensions and other physical characteristics are given in table I. All calculations were made for one flight condition, a Mach number of 0.7 and an altitude of 30,000 feet.

The stability derivatives for the airplane were estimated from unpublished data and are presented in table II. The airplane transfer functions relating pertinent response parameters to rudder and aileron deflections and to side-gust inputs were obtained in the manner described in reference 1. These transfer functions were then simplified by eliminating certain degrees of freedom. The validity of these simplifications for analysis of the present airplane-autopilot combination was checked in reference 1 by comparing results obtained by using the simplified concepts with those obtained by using the three-degree-of-freedom equations. Some sample three-degree-of-freedom responses to side gusts, with corresponding results obtained by the simplified analysis, are shown in figure 2. The agreement is felt to be satisfactory. The simplified transfer functions used are presented in table II.

Basic Autopilot

The basic autopilot considered herein is representative of a production type that is currently used in fighter airplanes. A block diagram of the airplane-autopilot system is presented in figure 3. Only the aileron and rudder channels of the autopilot were considered since only responses to side gusts were studied and since the longitudinal and lateral motions of the airplane were assumed to be uncoupled. The rudder channel incorporated yaw-rate feedback for damping of the Dutch roll oscillation and sideslip feedback for sideslip regulation. The aileron

channel incorporated roll-angle feedback to provide roll stability and, in addition, incorporated a heading signal to cause the airplane to roll in order to reduce heading errors. The block diagram shown in figure 4 is a simplified version of the complete basic airplane-autopilot system. This simplified system was used in the present analysis.

Gust-Compensating Autopilot

The response of the airplane-autopilot configuration shown in figure 3 has been studied previously (ref. 1), and the system has been found to have an undesirably large roll and yaw response to side gusts. The modified system shown in figure 5 is intended to alleviate these poor gust-response characteristics while maintaining the desirable command characteristics of the basic autopilot. A simplified version of the modified autopilot, presented in a block diagram in figure 6, was used for analysis. Two modifications, which consisted of passing the signal from the sideslip vane through a low-pass filter and of passing a yaw-rate signal through the same filter, were made in the rudder channel. (See fig. 5.) The resulting rudder channel has a dual-mode type of operation. The rudder regulates sideslip during commanded heading changes, but regulates heading during side-gust disturbances (except over some low band of frequencies determined by the filter time constant over which sideslip is regulated). Achievement of this operation is based on the assumption that the sideslip generated with respect to the stationary air mass β_o is equal to the negative of the yaw angle ψ. Except at low frequencies, this assumption very closely approximates a condition existing for current airplanes whose side forces are low in comparison to their weight. In more detail, what occurs in the rudder loop is that at low frequencies the yaw-rate signals are negligible and the sideslip signal is passed unattenuated through the filter. The primary purposes of the filter are to cut off the signal from the sideslip vane at high frequencies and to integrate the yawing-velocity signal at high frequencies, thereby providing heading regulation. In still air this integrated rate signal also provides regulation of sideslip, since, with respect to the stationary air mass, ψ is approximately equal to $-\beta$. A complete discussion of the filters of the type used in this investigation is presented in reference 2.

The relations between the feedback quantity in the outer loop of the rudder channel and the quantities ψ, β, and β_o may be developed analytically through reference to figure 5, and can be written

$$\bar{\beta} = \frac{\beta}{1 + \tau s} - \frac{\tau s \psi}{1 + \tau s} \tag{1}$$

For command inputs in still air (assuming that $\beta_o = -\psi$),

$$\beta = \beta_o$$

and

$$\overline{\beta} = \frac{\beta}{1 + \tau s} + \frac{\tau s \beta}{1 + \tau s} = \beta \tag{2}$$

Thus, sideslip is regulated at all frequencies.

For side-gust inputs (assuming that $\beta_o = -\psi$),

$$\beta = \beta_g + \beta_o$$

and

$$\overline{\beta} = \frac{\beta_g + \beta_o}{1 + \tau s} + \frac{\tau s \beta_o}{1 + \tau s} = \frac{\beta_g}{1 + \tau s} + \beta_o \tag{3}$$

Thus, sideslip due to side gusts is attenuated above some frequency determined by the time constant τ, whereas sideslip with respect to still air is regulated at all frequencies. Equation (1) from another viewpoint indicates that, for side-gust inputs, $\overline{\beta} = \beta$ as $\omega \rightarrow 0$ (sideslip is regulated) and $\overline{\beta} = -\psi$ as $\omega \rightarrow \infty$ (heading is regulated).

The extent to which the assumption that ψ equals $-\beta_o$ is valid for the airplane employed is illustrated in figure 7. The frequency responses of β_o and ψ to aileron, rudder, and side-gust inputs are compared. These frequency responses were obtained analytically by using estimated derivatives and three degrees of lateral freedom. The analytical approach was used because, in general, flight tests have not afforded accurate measurement of the response at the low frequencies where discrepancies between β_o and $-\psi$ occur. The comparison of the responses of β_o with $-\psi$ in figure 7 shows that, for side-gust inputs, good agreement exists at all frequencies and for control-deflection inputs, good agreement exists above a frequency of 1.5 radians per second.

Autopilot Gain Adjustments

In the calculations the autopilot servos were assumed to be perfect, and their transfer functions were represented by simple gains. This

assumption is reasonable if the autopilot-servo frequencies are high with respect to the natural frequencies of the airplane-autopilot system.

The gain of the sideslip loop was adjusted to quadruple the directional stability of the airplane without the autopilot. This stability augmentation resulted in approximately doubling the natural frequency of the airplane in yaw. The natural frequency (Dutch roll mode) of the airplane without the autopilot was about 3 radians per second.

The gain of the yaw-rate loop was adjusted so that the damping of the directional oscillation of the augmented airplane was sufficient to reduce the amplitude to 1/5 in 1 cycle. This degree of damping more than meets current requirements for flying qualities. The roll-angle gain used in the aileron channel was limited to the value at which the time to damp the rolling oscillation (introduced by the roll stability loop) was the same as that for the yawing oscillation. The frequency of roll oscillation was about 5 radians per second. No augmentation to the roll damping of the basic airplane was provided.

The gain of the heading signal applied to the aileron channel was made 10 times larger than the roll-angle gain. This gain relationship resulted in a steady-state bank angle of 10° for each degree of heading error and provided a moderately rapid change in the course of the airplane following a heading command.

The gain of the yaw-rate signal fed to the filter of the compensated rudder channel was made equal to the filter time constant. This adjustment resulted in compensation not affecting the performance of the sideslip loop during command maneuvers in still air and provided the same loop gain for heading regulation during side-gust disturbances as that which existed for the sideslip regulation in command maneuvers. The filter time constant itself was a variable in the analysis. The investigated range of this time constant was from 0 to 5 seconds.

The gain values chosen for the various loops are presented in the following table:

K_r, radians/radian/sec	0.5
K_β, radians/radian	5
K_ϕ, radians/radian	1
K_ψ, radians/radian	10
τ, sec	0, 1, 2, 5

METHOD OF ANALYSIS

The transfer functions relating the roll and yaw responses of the airplane-autopilot combination to side gusts were determined in a manner similar to that described in reference 1. The general approach used was that described in standard textbooks on servomechanisms. (See ref. 3, for example.) The frequency responses to side gusts of the airplane motions were determined by substituting $i\omega$ for s in the system transfer functions. The amplitude variation with frequency of the response to atmospheric turbulence was determined by multiplying the amplitude ratio of the frequency response by the square root of the power spectral density of the side-gust component of the atmospheric turbulence. The power spectral density of side gusts was derived from reference 4.

The amplitude of the power spectral density of side gusts is shown to vary as the inverse square of the frequency. The overall level of the amplitude is dependent on the intensity of the turbulence. The present analysis, however, is concerned solely with the frequency variation of the airplane response.

RESULTS

Airplane With Basic Autopilot

The frequency responses to side gusts of the airplane in combination with the original autopilot are presented in figure 8. The yaw, sideslip, and roll responses are shown. Although rolling gusts will also produce disturbances to the lateral motion of an airplane, the results reported in reference 1 show that the rolling-gust disturbances were, in general, much smaller than the side-gust disturbances; therefore, only the latter disturbances are considered herein. For purposes of comparison, the corresponding frequency responses of the airplane without the autopilot are also presented in figure 8.

The responses of the airplane without the autopilot exhibit a very sharp resonance peak which reflects the low damping of the Dutch roll oscillation of the airplane. With the autopilot installed, the yaw-damper component very effectively reduces this resonance peak. In addition, the sideslip-regulation component causes the airplane to yaw into the gust with greater tightness than exists with the airplane alone. This result is indicated by the delay to higher frequencies of the buildup in the sideslip responses and by the higher peak frequency of the yaw response when the autopilot is used.

With the autopilot in operation, the amplitude of the roll motion in response to side gusts is very large. This result stems from the moderately large amplitude of the yaw motion in response to side gusts and the strong coupling between roll and yaw supplied by the autopilot. As mentioned previously, the static ratio of roll to yaw was 10 with the autopilot-equipped airplane. The roll response could be reduced by reducing the gain of the yaw signal fed into the aileron channel, but this change would proportionately reduce the speed of response to heading commands. Such possibilities are discussed in the section entitled "Discussion."

Airplane With Gust-Compensating Autopilot

The frequency responses to side gusts of the airplane in combination with the gust-compensating autopilot are presented in figure 9. The yaw, sideslip, and roll responses are shown for values of the filter time constant of the compensating system of 0, 1, 2, and 5 seconds. The original autopilot corresponds to a filter time constant τ equal to zero. Corresponding plots showing the statistical amplitude variation with frequency of the response to actual turbulence are presented in figure 10. No amplitude scales are given in this figure because it is beyond the scope of the present study to predict the actual amplitudes for any given atmospheric condition; however, the relative magnitude of the response of the different systems can be inferred from these curves. In addition, the relative magnitudes of the roll, yaw, and sideslip motions can be established from such calculations. In this connection, the calculated values of yaw and sideslip were increased by a factor of 5 for presentation in figure 10 because the importance of the yawing and sideslipping motions relative to the rolling motions is believed to be represented approximately by this factor. The curves are terminated at the low-frequency end at approximately $\omega = 0.7$ radian per second. Recent measurements have shown that the inverse-square variation of the power spectral density of side gusts holds true for gust wavelengths up to 6,000 feet (which corresponds to a frequency of $\omega = 0.7$ radian per second for the conditions assumed in this paper). For longer gust wavelengths, the slope of this curve is reduced and, eventually, the slope of the power-spectral-density curve goes to zero.

Both figures 9 and 10 show that, except over some low band of frequencies, there is a marked reduction in the amplitude of the roll and yaw response to side gusts when the compensation is used. At the peak frequency of the uncompensated system, the amplitude of these responses of the gust-compensating system is about 30 percent of that of the uncompensated system. The reduction is somewhat smaller at lower frequencies and generally somewhat greater at higher frequencies. At low frequencies the behavior of the compensated system approaches that of the uncompensated system and sideslip regulation occurs. The frequency

band over which this condition exists can be varied by varying the filter time constant. Even with the use of the gust-compensating autopilot, the amplitude of the response to the atmospheric turbulence shows a pronounced tendency to rise at the lower frequencies. This result stems from the inverse-square frequency variation of the power spectrum of side gusts. Increase in the filter time constant alleviates this tendency.

In order to complete the presentation of system response, the heading responses to heading commands for the airplane-autopilot system are presented in figure 11. These responses were obtained by the method presented in reference 1 and are shown both for a roll-yaw coupling of 10 (the same as that used for the side-gust calculations) and for a roll-yaw coupling of three. In the the former case, the break frequency (the frequency at which response rapidly departs from unity) is about 0.45 radian per second; whereas in the latter case, the break frequency is reduced to about 0.15 radian per second. The inverse of the break-frequency value represents the time required to reduce a heading error to roughly one-third of its initial value. Within the limits of the assumptions, the command responses of the gust-compensating autopilot and the original autopilot are the same.

DISCUSSION

Many current and proposed autopilots utilize the principle of the autopilot used in the present study of applying heading commands to the aileron channel. This approach is employed because a system which causes the airplane to roll in response to steering error provides the only practical way, in an airplane configuration, to have course changes closely follow heading changes, since the only effective method of changing the course of an airplane is to tilt the lift vector. By applying heading commands to the aileron channel, the rudder channel can be used for sideslip regulation. This system, therefore, provides both increased directional stability and improved coordination during turning maneuvers. In homing systems, such as automatic interceptors, in which the steering information is obtained from radar tracking-line information, the lateral-steering command invariably goes directly or indirectly into the aileron channel. In rocket-firing interceptors, where velocity-jump corrections are large, rapid response in path to steering error and tight sideslip regulation are particularly important.

In the system considered herein, if the sideslip is regulated perfectly, the course and heading response to lateral-steering commands are the same; however, in order to obtain even a moderately rapid response, a fairly large roll angle must result from heading errors. The frequency response presented in figure 11 for a roll-to-yaw ratio of 10 corresponds to a response time (time for an indicial error to be

reduced to 1/20) of about 7 seconds. For a roll-to-yaw ratio of 3 the response time is over 20 seconds.

In order to evaluate the usefulness of the airplane-autopilot combination, consideration must be given to the response to external disturbances such as gusts as well as to the response to commands. It appears that any system designed to provide rapid course response and to minimize sideslip would be expected to have an undesirably large roll response due to side gusts (because of the high required ratio of roll to yaw) unless special measures are incorporated to alleviate this problem.

The approach examined herein still utilizes a high roll-to-yaw coupling in the autopilot but alleviates the effects of side-gust disturbances by the simple expedient of keeping the airplane from yawing into the gust. Within the limits that $\psi = -\beta_o$, the frequency response in heading to heading commands of the gust-compensating airplane-autopilot system should not differ from the response of the original system shown in figure 11.

Although sideslip regulation during high-frequency gust disturbances no longer exists in the gust-compensating autopilot, there is no apparent reason why such regulation is desirable. Even in rocket firing it does not appear desirable to regulate the sideslip produced by gusts having periods which are short compared with the response time of the lateral-steering system, since control of sideslip under these conditions would result in throwing the launcher line off the target. A similar result appears true in automatic landings. In both cases it does appear desirable to regulate sideslip due to gusts below some low value of frequency, and it may be noted that the compensating autopilot provides this feature. This latter characteristic does tend to produce larger yawing and rolling amplitudes in the low-frequency range; however, because of the low frequency associated with these motions, these larger amplitudes may not be objectionable in most operations.

Although the magnitudes of these motions can be reduced by increasing the filter time constant, the value of the time constant may be limited by such factors as achievement of desirable characteristics during turns. For example, if the filter time constant is allowed to become very large, the gust-compensating autopilot will approach a system wherein heading is regulated in both the roll and yaw channels at all frequencies. (See figs. 6, 9(a), and 10(a).) With this situation a heading command would cause the airplane to roll, but at the same time the rudder channel would operate also to yaw the airplane in order to reduce the heading error. This mode of rudder operation would tend to uncoordinate the turn. If sideslip signals were not provided and only high-frequency heading signals were allowed to pass in the rudder channel, this uncoordinated signal would be avoided, but no improvement in the rudder—fixed-turn coordination

of the basic airplane would be afforded. Providing low-frequency sideslip signals in the rudder channel affords improvement in the turn coordination. These characteristics are inherent in the system described herein, and the essential features could be mechanized also by several other means. With regard to the present system, it appears that flight experience would be useful in establishing the most suitable value of the filter time constant.

In many current autopilots, improved turn coordination is obtained through regulation of side force rather than sideslip. Apparently, the use of side-force regulation stems primarily from the ease with which a side-force measurement can be mechanized. The gust-compensating plan discussed herein is equally applicable where side force is the feedback quantity in the outer loop of the rudder channel. In this case, in accordance with the operation outlined in the section entitled "Gust-Compensating Autopilot," side force would be regulated at low frequencies for both gusts and command inputs, whereas heading (and sideslip for command inputs) would be regulated at high frequencies.

CONCLUDING REMARKS

A previous study (NACA TN 3603) showed that the basic type of airplane-autopilot system investigated in the present paper provided a good course response to lateral-steering commands and greatly reduced the gust response of the Dutch roll mode, but that, in its basic form, the system had undesirably large side-gust responses in roll and yaw over a wide frequency range. The present study, which is applied to a given flight condition, shows that compensation for side gusts applied solely to the rudder channel materially reduced these gust responses without affecting the command response. Some further work to establish the detailed operating characteristics of the gust-compensating system at low frequencies appears warranted.

Langley Aeronautical Laboratory,
National Advisory Committee for Aeronautics,
Langley Field, Va., December 29, 1955.

REFERENCES

1. Adams, James J., and Mathews, Charles W.: Theoretical Study of the Lateral Frequency Response to Gusts of a Fighter Airplane, Both With Controls Fixed and With Several Types of Autopilots. NACA TN 3603, 1956.

2. James, Hubert M., Nichols, Nathaniel B., and Phillips, Ralph S.: Theory of Servomechanisms. McGraw-Hill Book Co., Inc., 1947, pp. 24-30.

3. Chestnut, Harold, and Mayer, Robert W.: Servomechanisms and Regulating System Design. Vol. I. John Wiley & Sons, Inc., 1951.

4. Summers, Robert A.: A Statistical Description of Large-Scale Atmospheric Turbulence. Sc. D. Thesis, M.I.T., 1954. (Also Rep. T-55, Instrumentation Lab., M.I.T., May 17, 1954.)

TABLE I

CHARACTERISTICS OF AIRPLANE USED IN CALCULATIONS

Physical characteristics:	
Weight, lb	12,600
Radius of gyration, k_X, ft	4.30
Radius of gyration, k_Z, ft	7.91
Wing area, sq ft	250
Vertical-tail area, sq ft	55
Wing span, ft	35.25
Horizontal-tail length, ft	15
Distance from thrust line to center of area of vertical tail, ft	5.32
Flight conditions:	
Airspeed, ft/sec	695
Altitude, ft	30,000
Mach number	0.7
Nondimensional data:	
μ	50
l_X	0.42
l_Z	0.112
K_X^2	0.01485
K_Z^2	0.0504
K_{XZ}	-0.00062
C_L	0.242

TABLE II

AIRPLANE STABILITY PARAMETERS

Stability derivatives:

C_{Y_β}	-0.58	$C_{n_{D^2\phi}}$	0.0147
$C_{Y_{D\beta}}$	0	$C_{n_{D_{p_t}}}$	0.0204
C_{Y_r}	0.45	$C_{n_{\delta_r}}$	-0.077
$C_{Y_{p_{wb}}}$	0	C_{l_β}	-0.115
$C_{Y_{p_t}}$	-0.013	$C_{l_{D\beta}}$	0
$C_{Y_{D^2\phi}}$	-0.0446	$C_{l_{r_{wb}}}$	0.004
$C_{Y_{D_{p_t}}}$	-0.050	$C_{l_{r_t}}$	0.05
C_{n_β}	0.12	$C_{l_{p_{wb}}}$	-0.45
$C_{n_{D\beta}}$	0	$C_{l_{p_t}}$	0
C_{n_r}	-0.147	$C_{l_{D^2\phi}}$	-0.005
$C_{n_{p_{wb}}}$	-0.039	$C_{l_{Dp_t}}$	-0.005
$C_{n_{p_t}}$	0.004	$C_{l_{\delta_a}}$	-0.086

$$\frac{\partial\sigma}{\partial\beta} = 0 \qquad \frac{\partial\sigma}{\partial D\phi} = 0.1$$

Transfer functions:

$$\frac{\psi}{\delta_r} = \frac{C_{n_{\delta_r}}}{2\mu K_Z^2 D^2 - \frac{1}{2} C_{n_r} D + C_{n_\beta}} = \frac{-0.077}{0.0130s^2 + 0.00373s + 0.12}$$

$$\frac{\psi}{\beta_g} = \frac{C_{n_\beta} + \frac{1}{2} C_{n_r} D}{2\mu K_Z^2 D^2 - \frac{1}{2} C_{n_r} D + C_{n_\beta}} = \frac{0.12 - 0.00373s}{0.0130s^2 + 0.00373s + 0.12}$$

$$\frac{\phi}{\delta_a} = \frac{C_{l_{\delta_a}}}{2\mu K_X^2 D^2 - \frac{1}{2} C_{l_p} D} = \frac{0.086}{0.00382s^2 + 0.0114s}$$

$$\frac{\phi}{\beta} = \frac{C_{l_\beta}}{2\mu K_X^2 D^2 - \frac{1}{2} C_{l_p} D} = \frac{-0.115}{0.00382s^2 + 0.0114s}$$

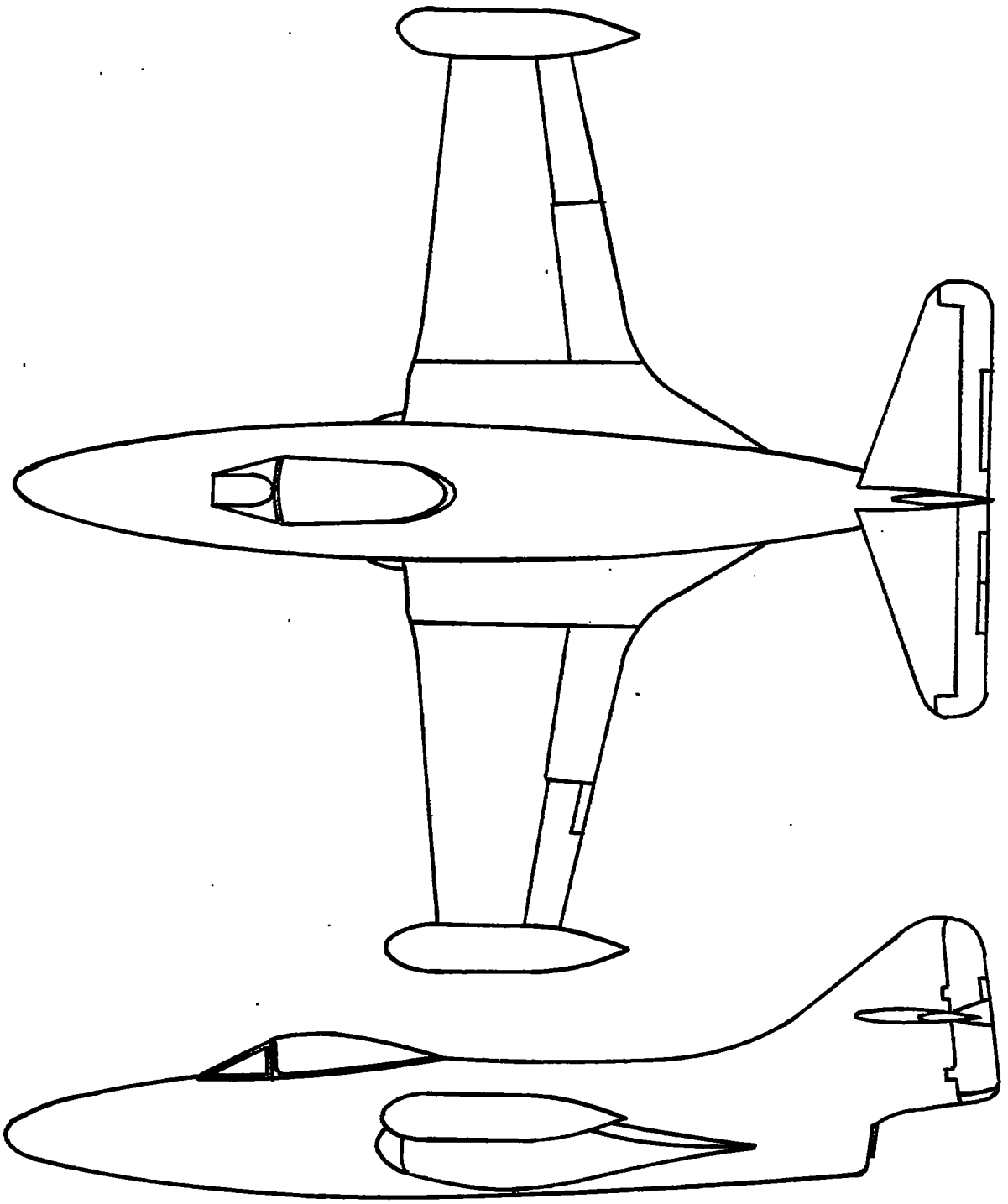

Figure 1.- Two-view drawing of airplane employed.

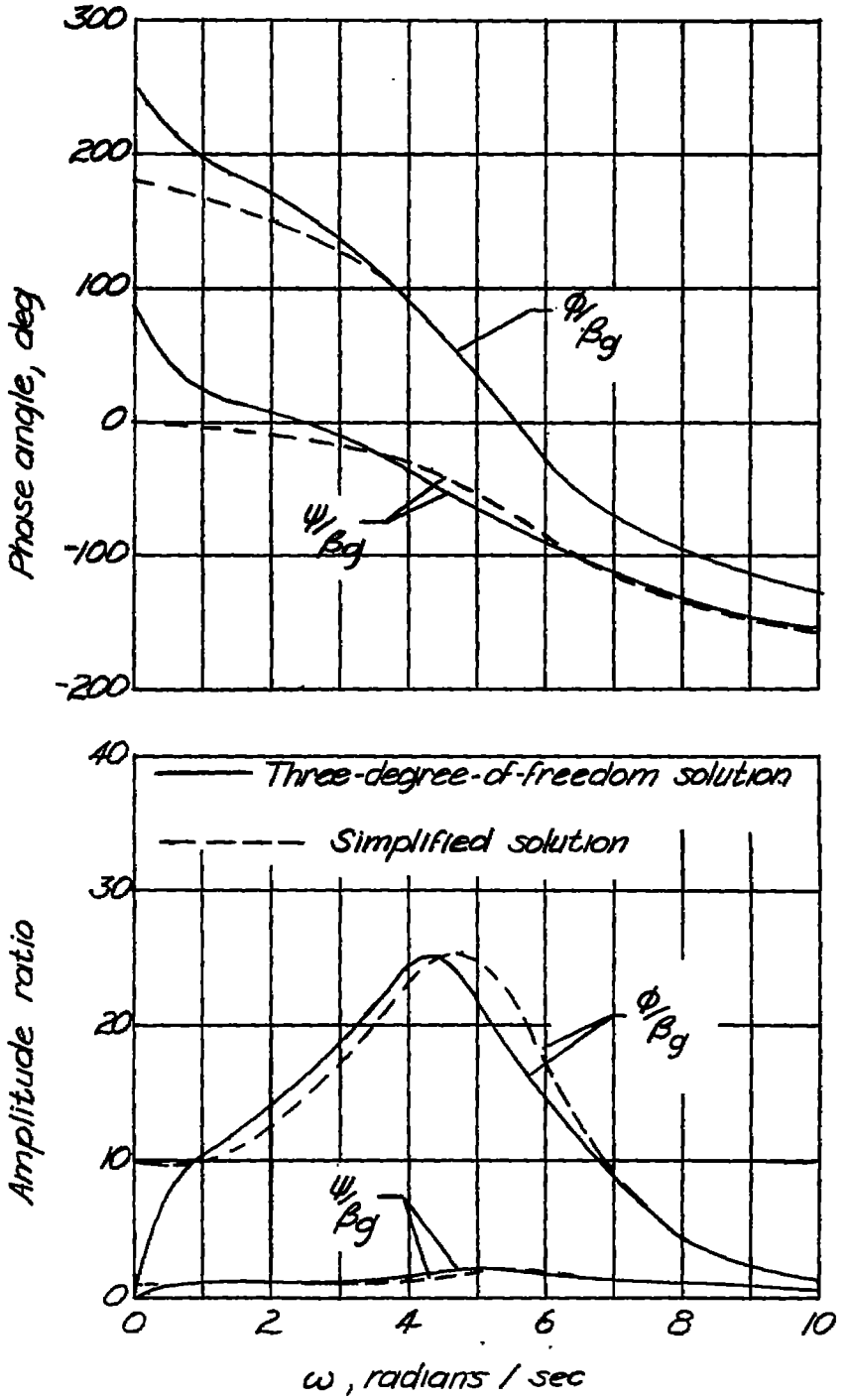

Figure 2.- Frequency response of the airplane in combination with the basic autopilot. The comparison is shown between the results obtained by using a three-degree-of-freedom analysis and the simplified analysis used in this paper.

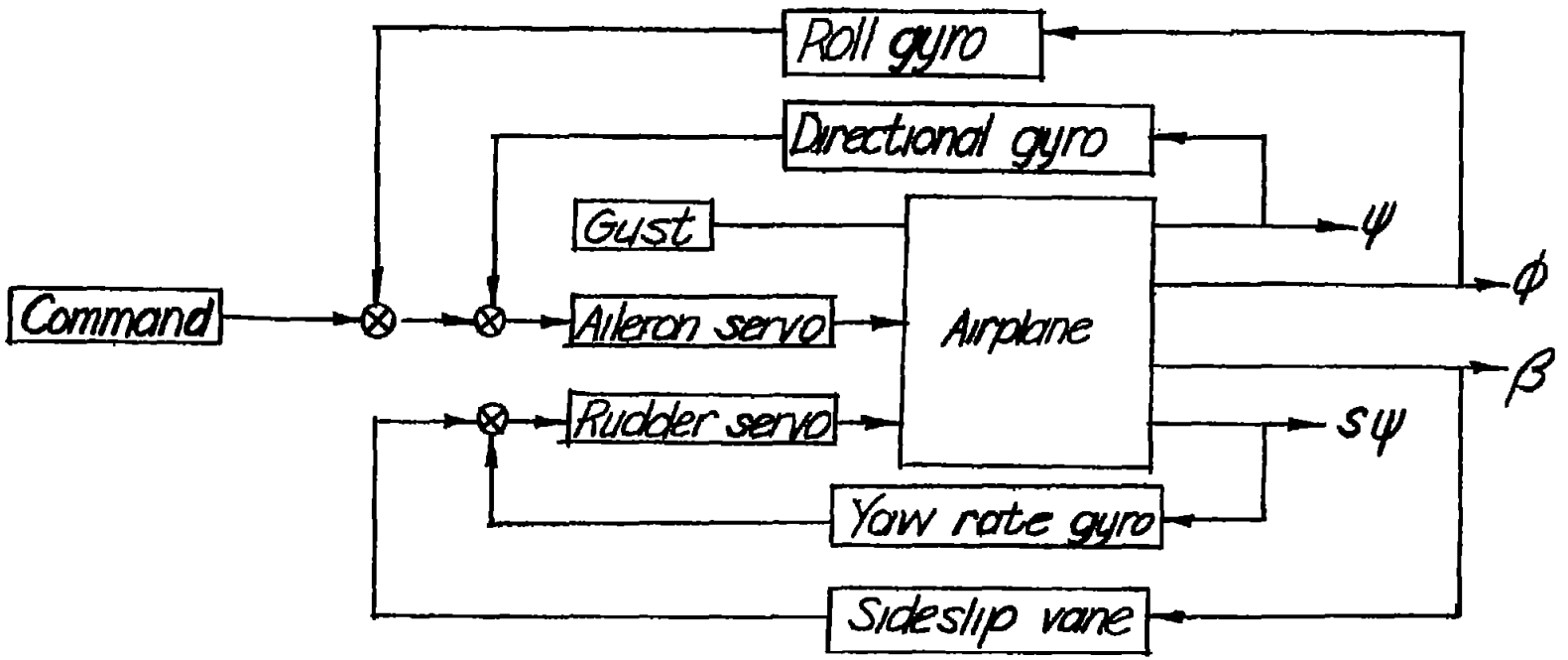

Figure 3.- Block diagram of basic airplane-autopilot system.

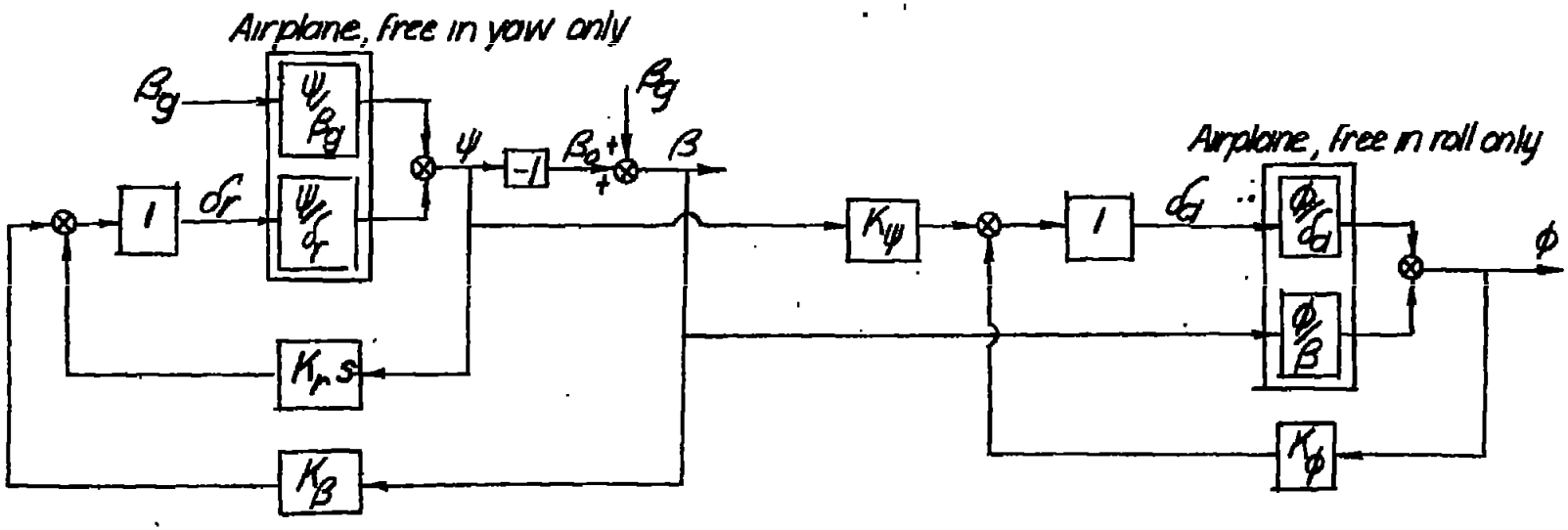

Figure 4.- Block diagram of simplified version of basic airplane-autopilot system.

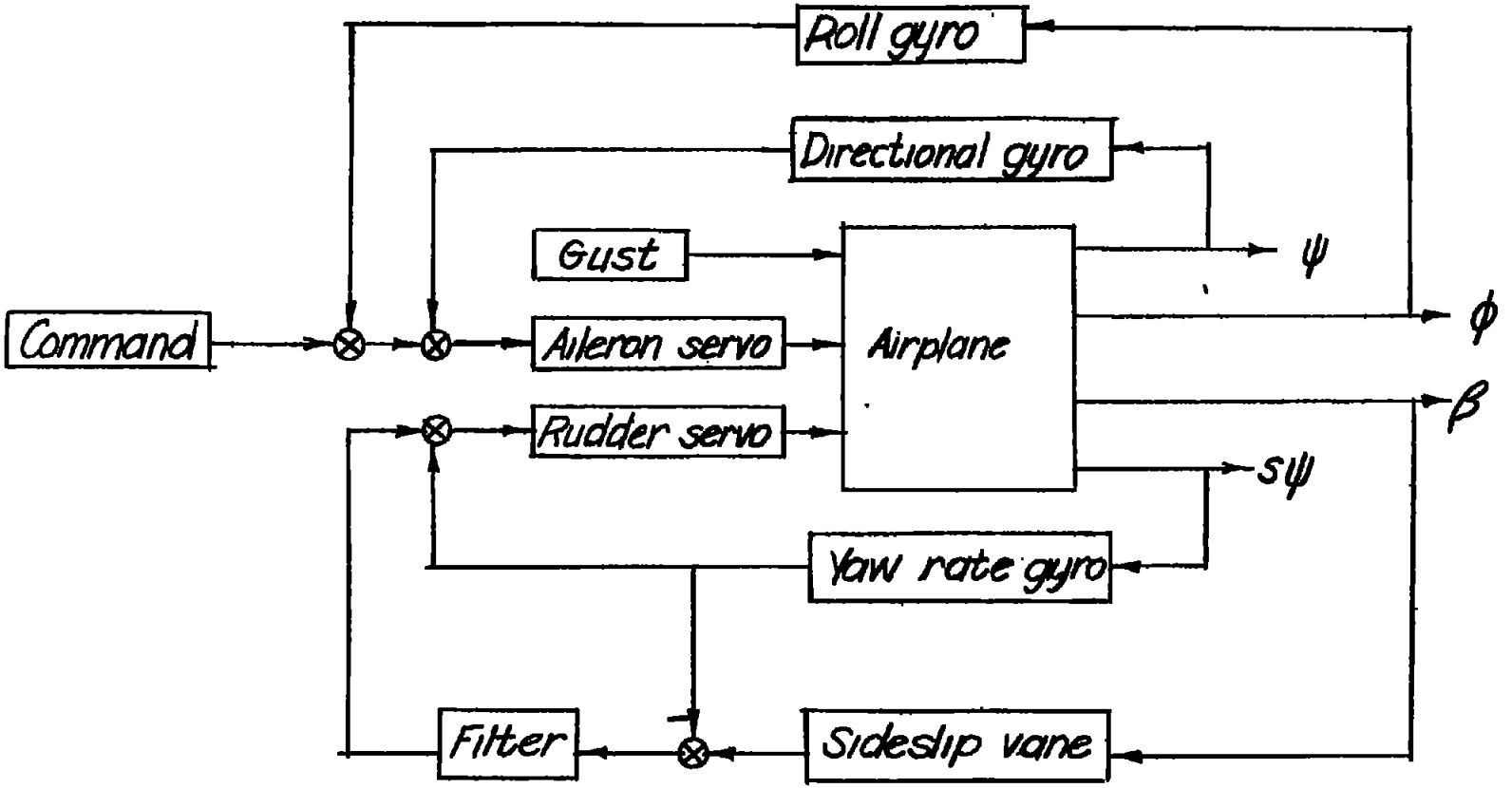

Figure 5.- Block diagram of gust-compensating airplane-autopilot system.

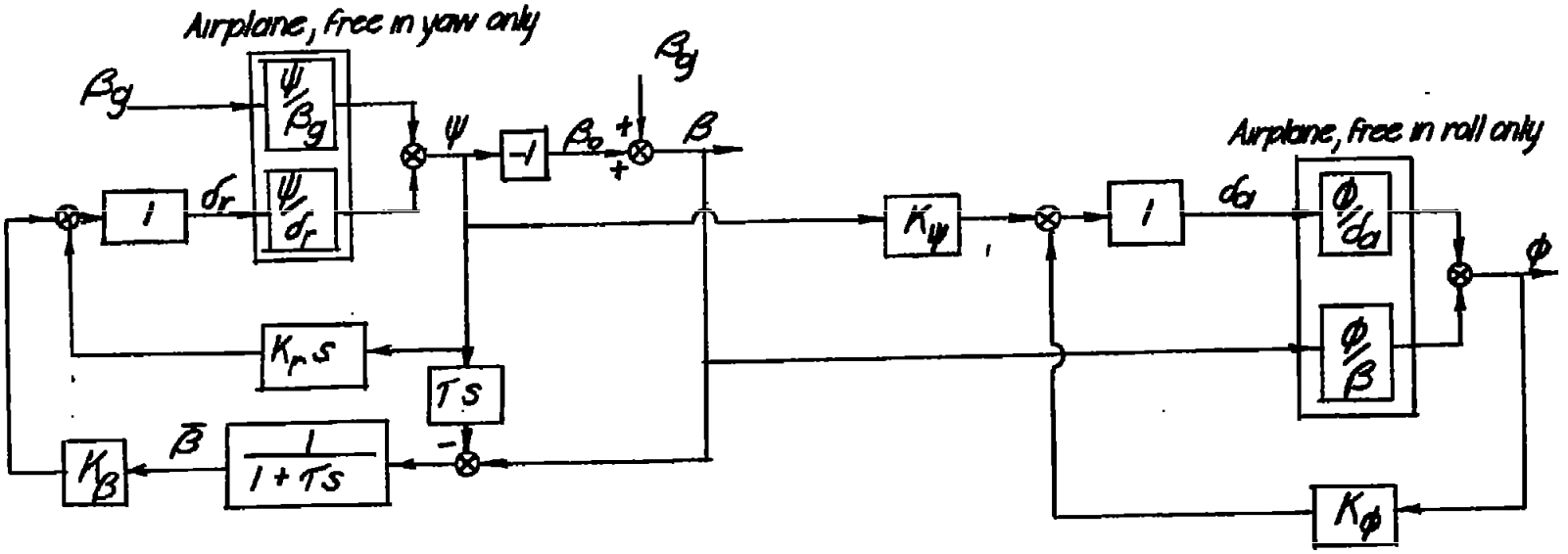

Figure 6.- Block diagram of simplified version of gust-compensating airplane-autopilot system.

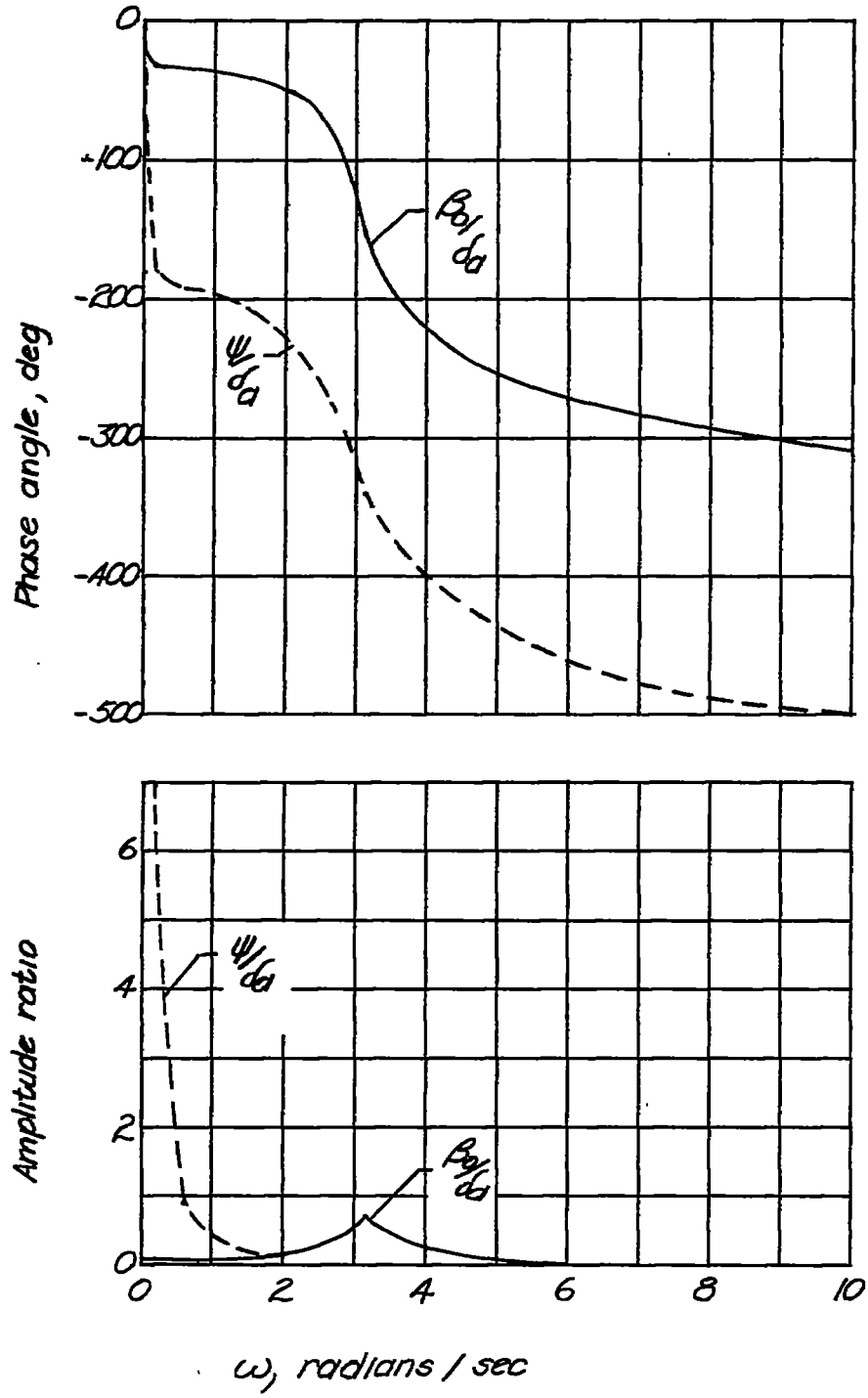

(a) Frequency responses of airplane to aileron deflection.

Figure 7.- Three-degree-of-freedom frequency responses of airplane showing comparison between ψ and β_o and responses to aileron, rudder, and side-gust inputs.

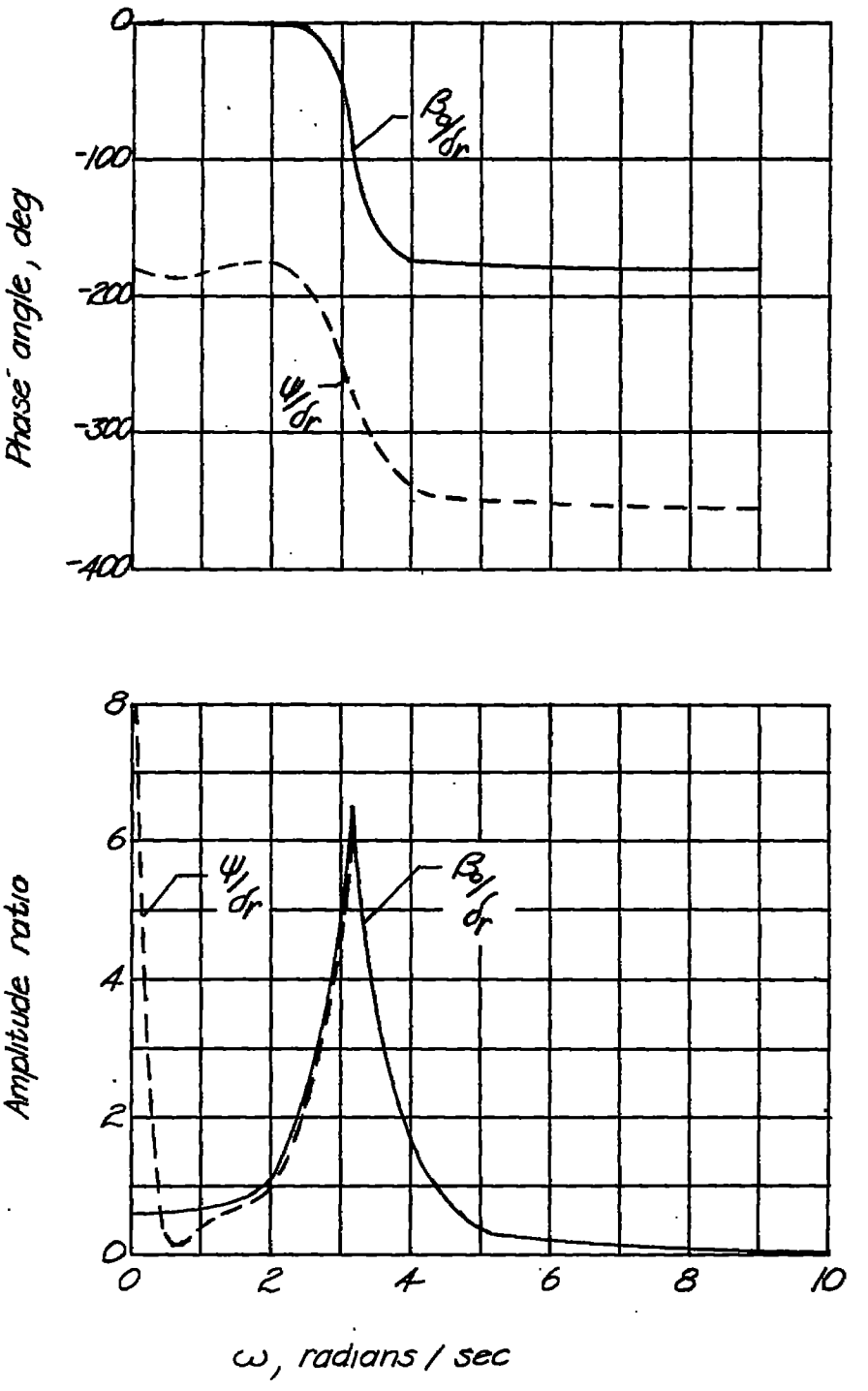

(b) Frequency responses of airplane to rudder deflection.

Figure 7.- Continued.

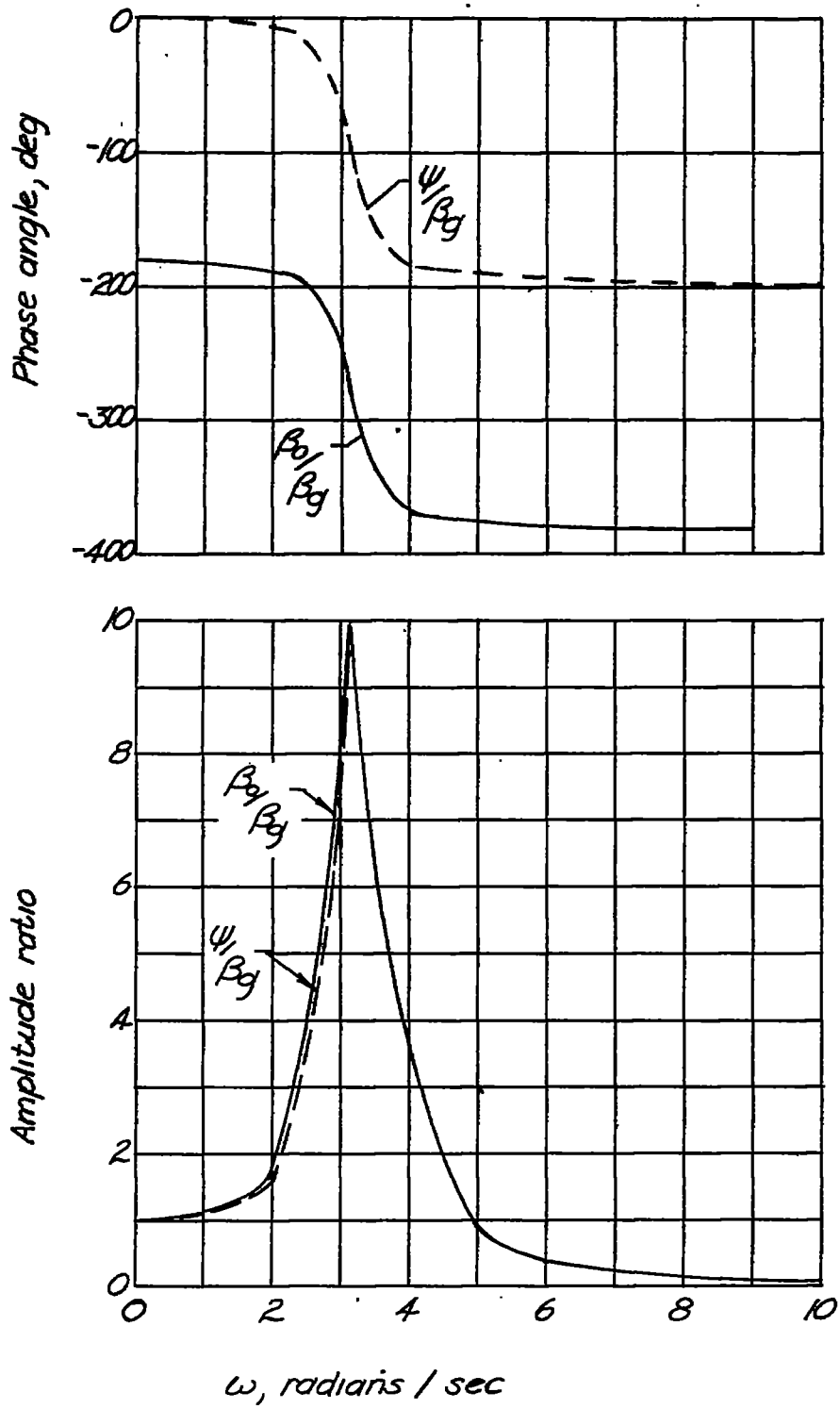

(c) Frequency responses of airplane to side gusts.

Figure 7.- Concluded.

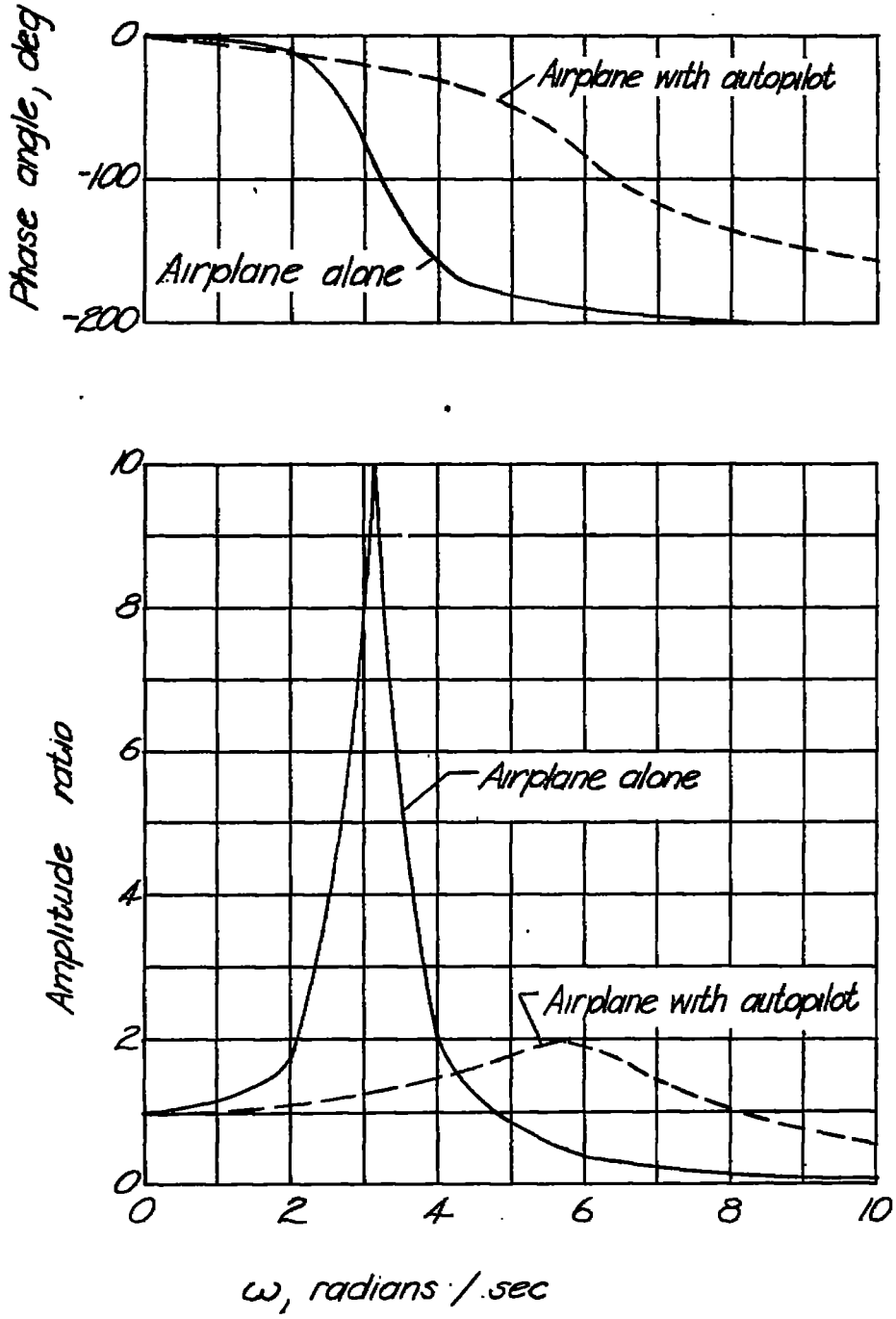

(a) Response of yaw angle ψ to side gusts β_g.

Figure 8.- Frequency responses to side gusts of airplane alone (airplane without autopilot) and of airplane in combination with basic autopilot. The effect of the original autopilot on the airplane response is shown.

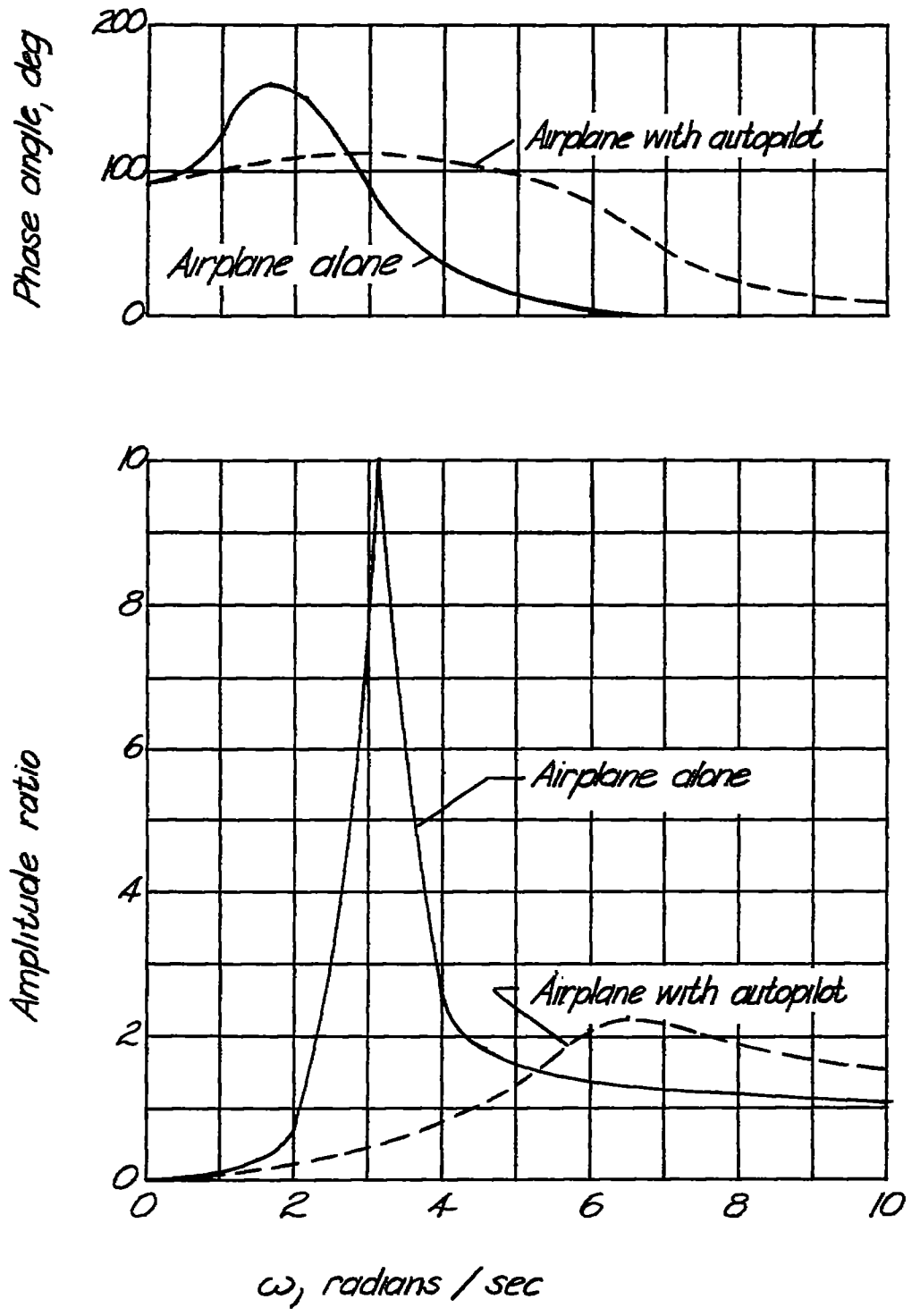

(b) Response of sideslip β to side gusts β_g.

Figure 8.- Continued.

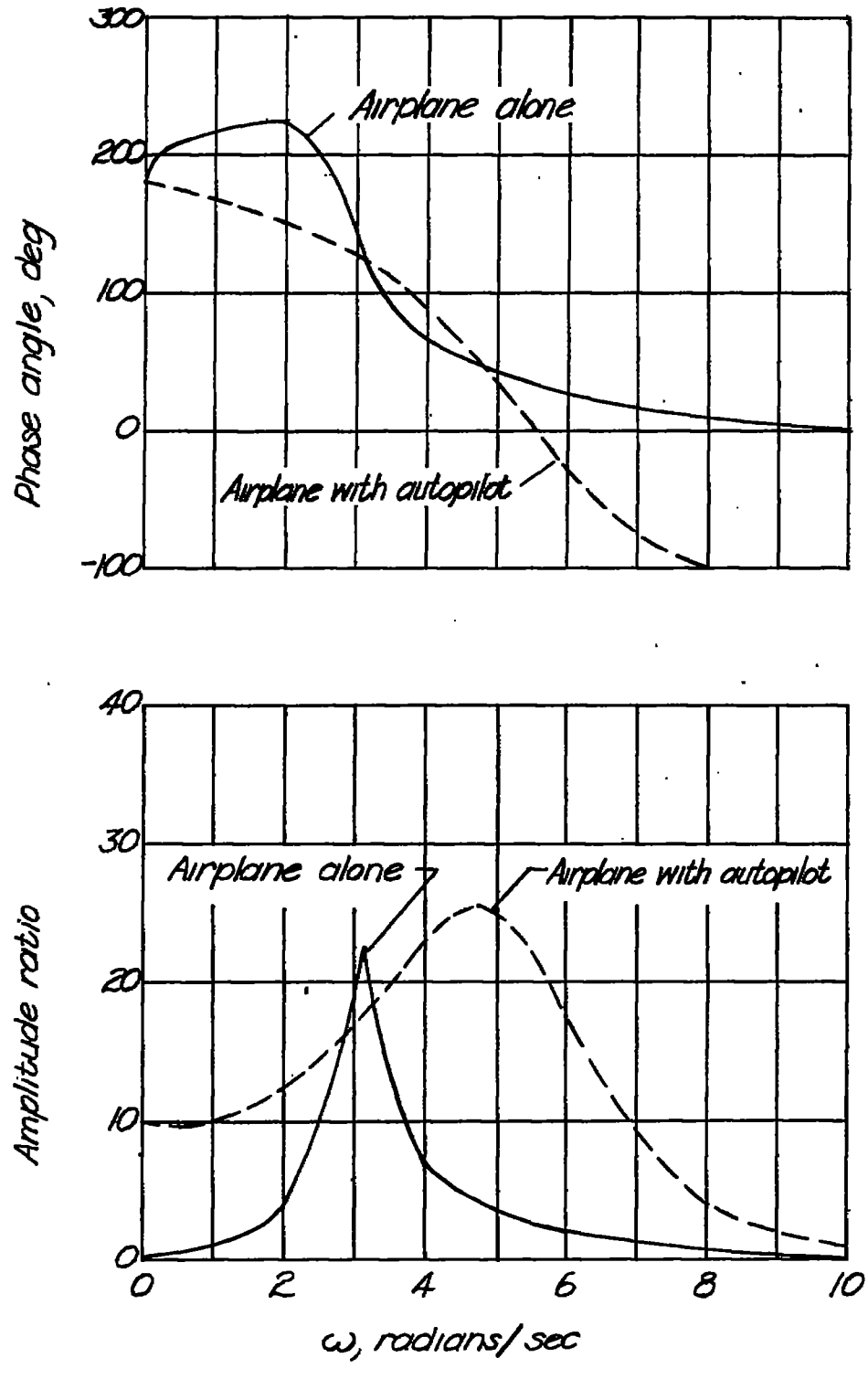

(c) Response of roll angle ϕ to side gusts β_g.

Figure 8.- Concluded.

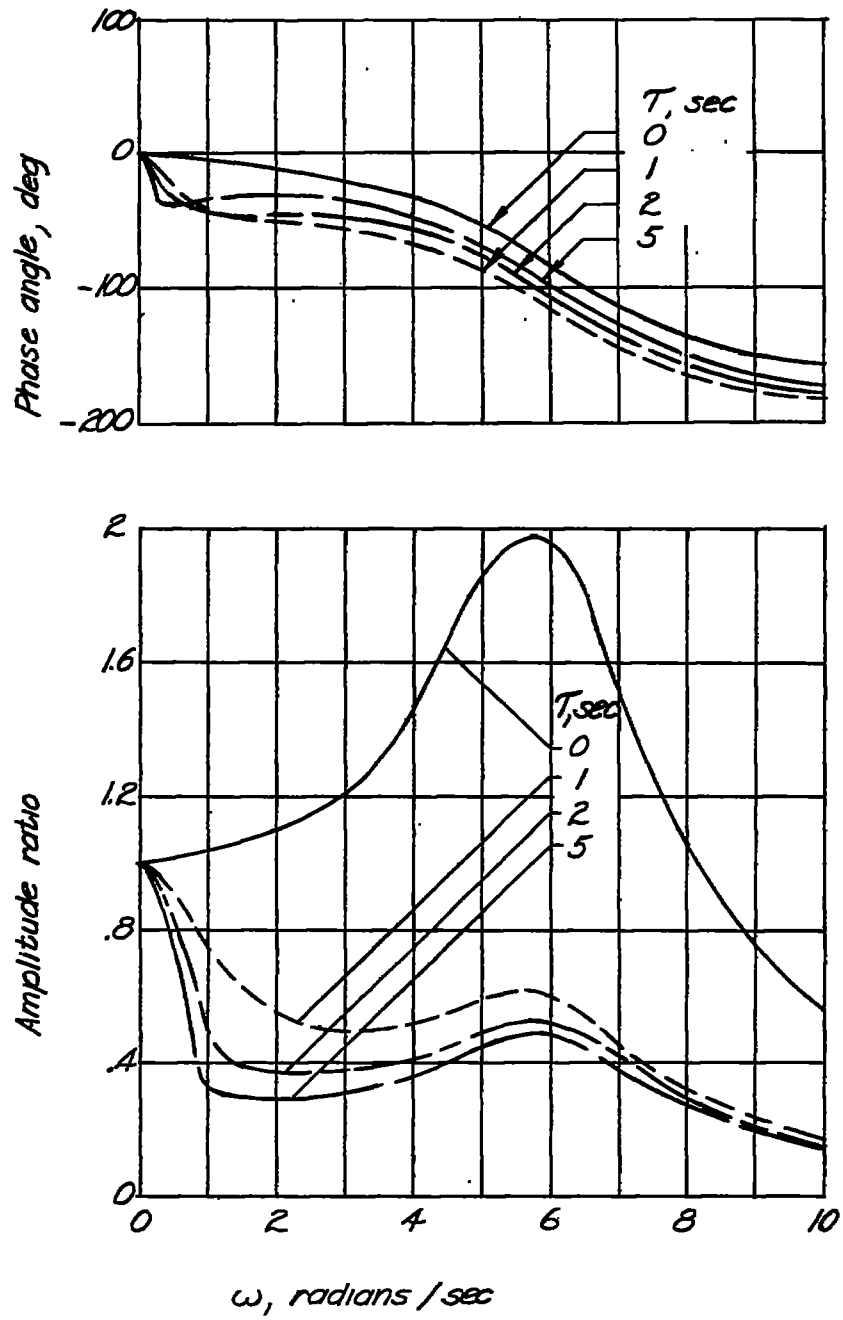

(a) Response of yaw angle ψ to side gusts β_g.

Figure 9.- Frequency responses of the airplane-autopilot system to side gusts for various values of the filter time constant of the gust-compensating autopilot system. The response of the original airplane-autopilot system is compared with the gust-compensating airplane-autopilot system. Original autopilot corresponds to $\tau = 0$.

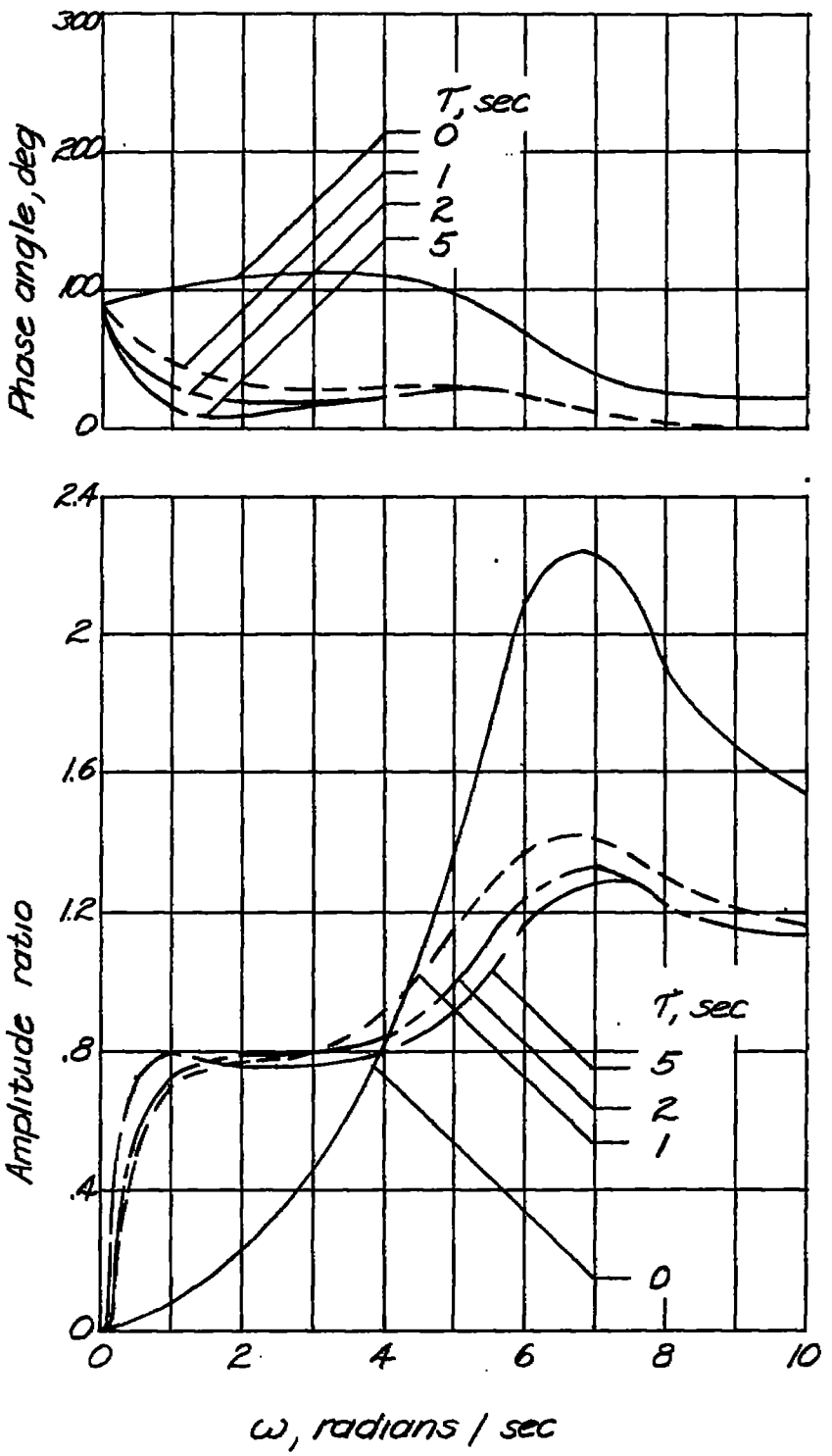

(b) Response of sideslip β to side gusts β_g.

Figure 9.- Continued.

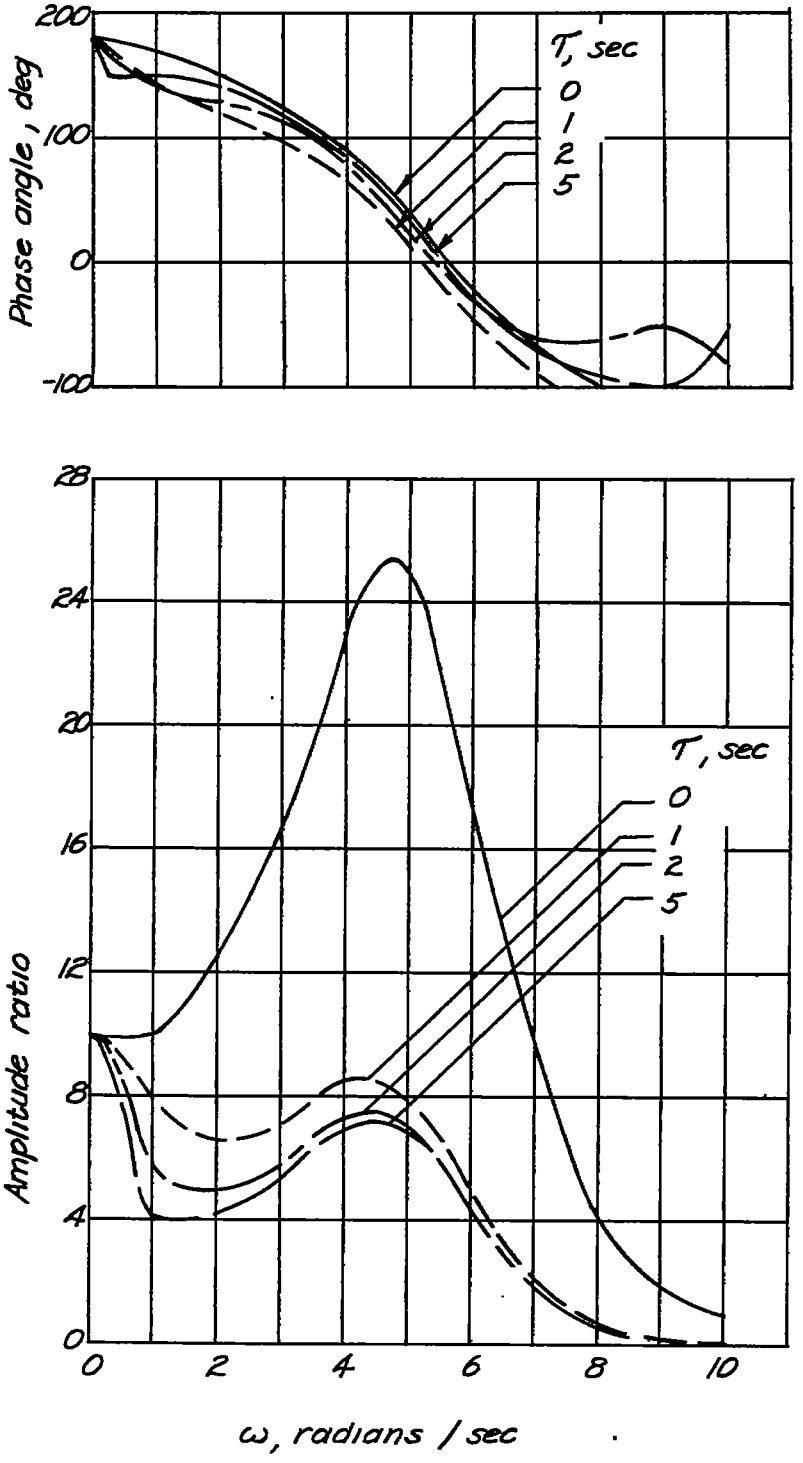

(c) Response of roll angle ϕ to side gusts β_g.

Figure 9.- Concluded.

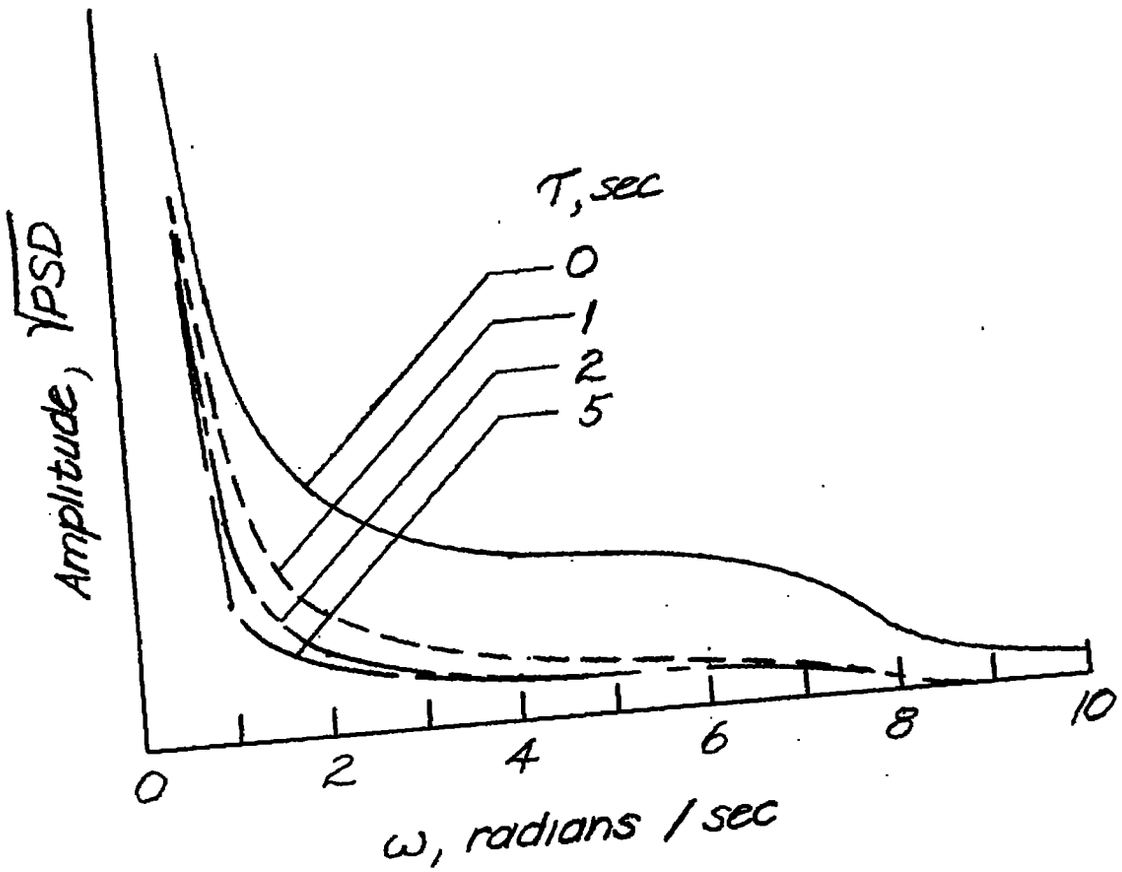

(a) Amplitude variation of yaw angle ψ with frequency.

Figure 10.- Amplitude variation with frequency of motion of the gust-compensating airplane-autopilot system when disturbed by the side-gust component of atmospheric turbulence. The amplitudes of ψ and β are presented with five times the scale of the amplitude of ϕ.

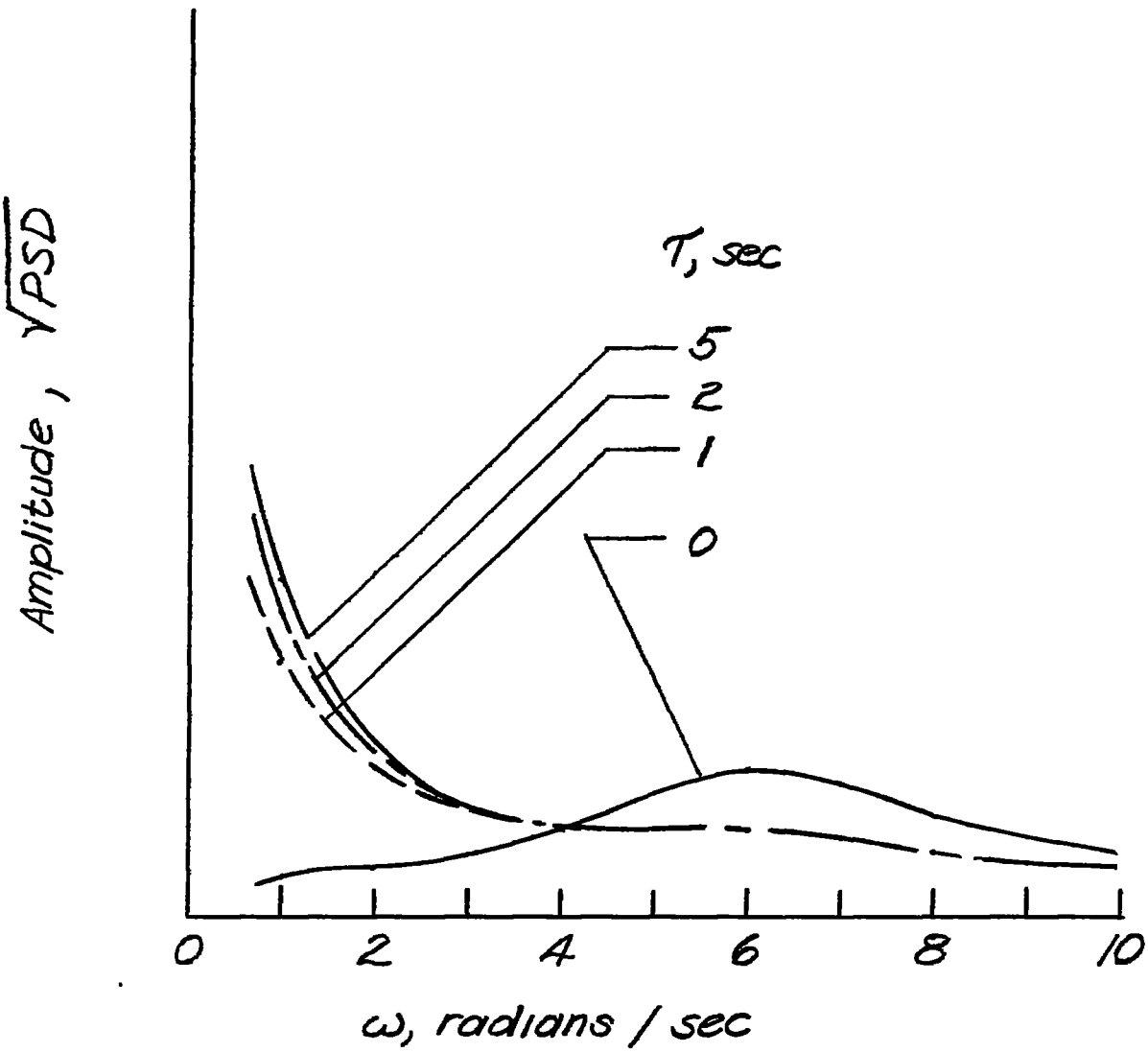

(b) Amplitude variation of sideslip angle β with frequency.

Figure 10.- Continued.

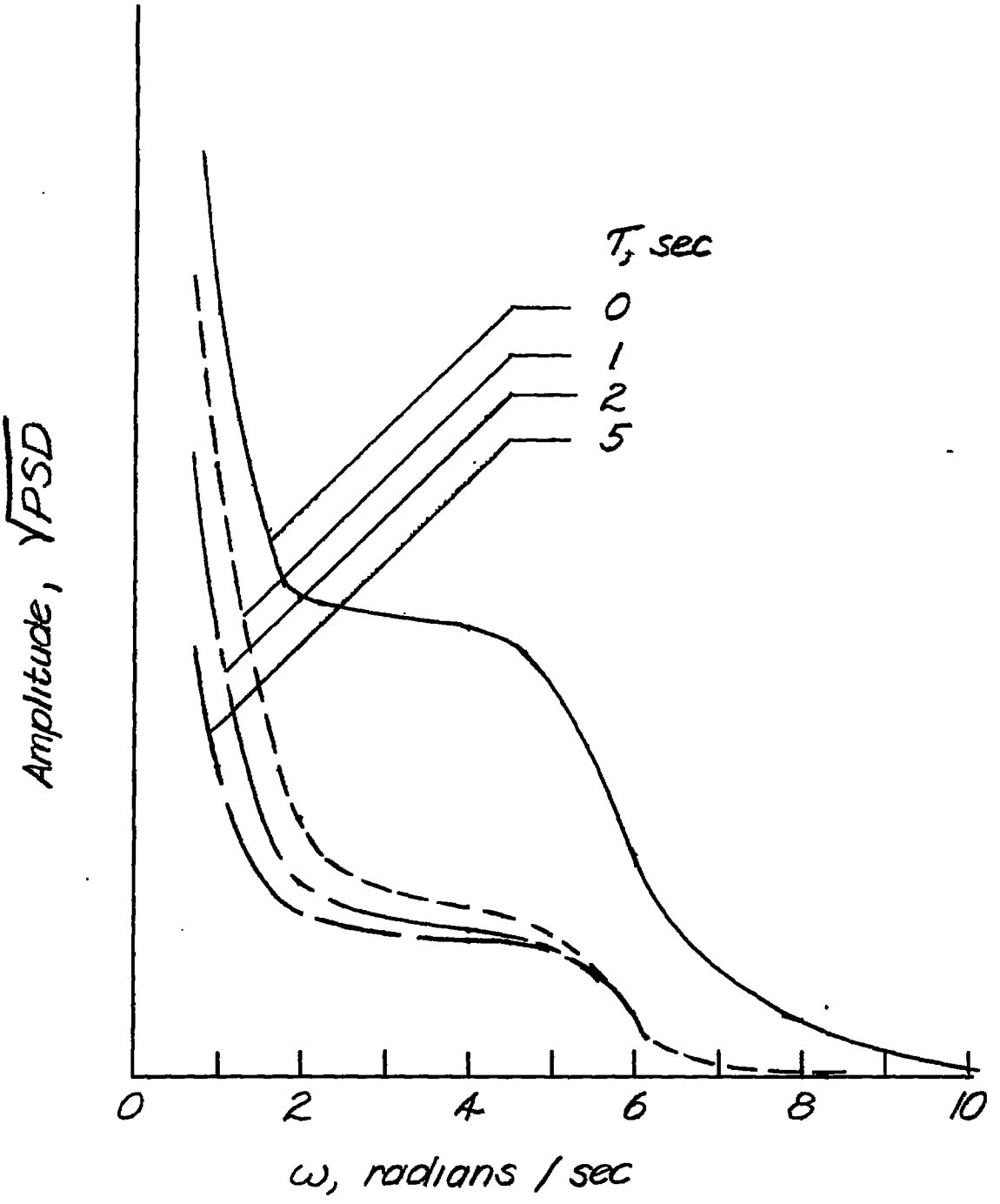

(c) Amplitude variation of roll angle ϕ with frequency.

Figure 10.- Concluded.

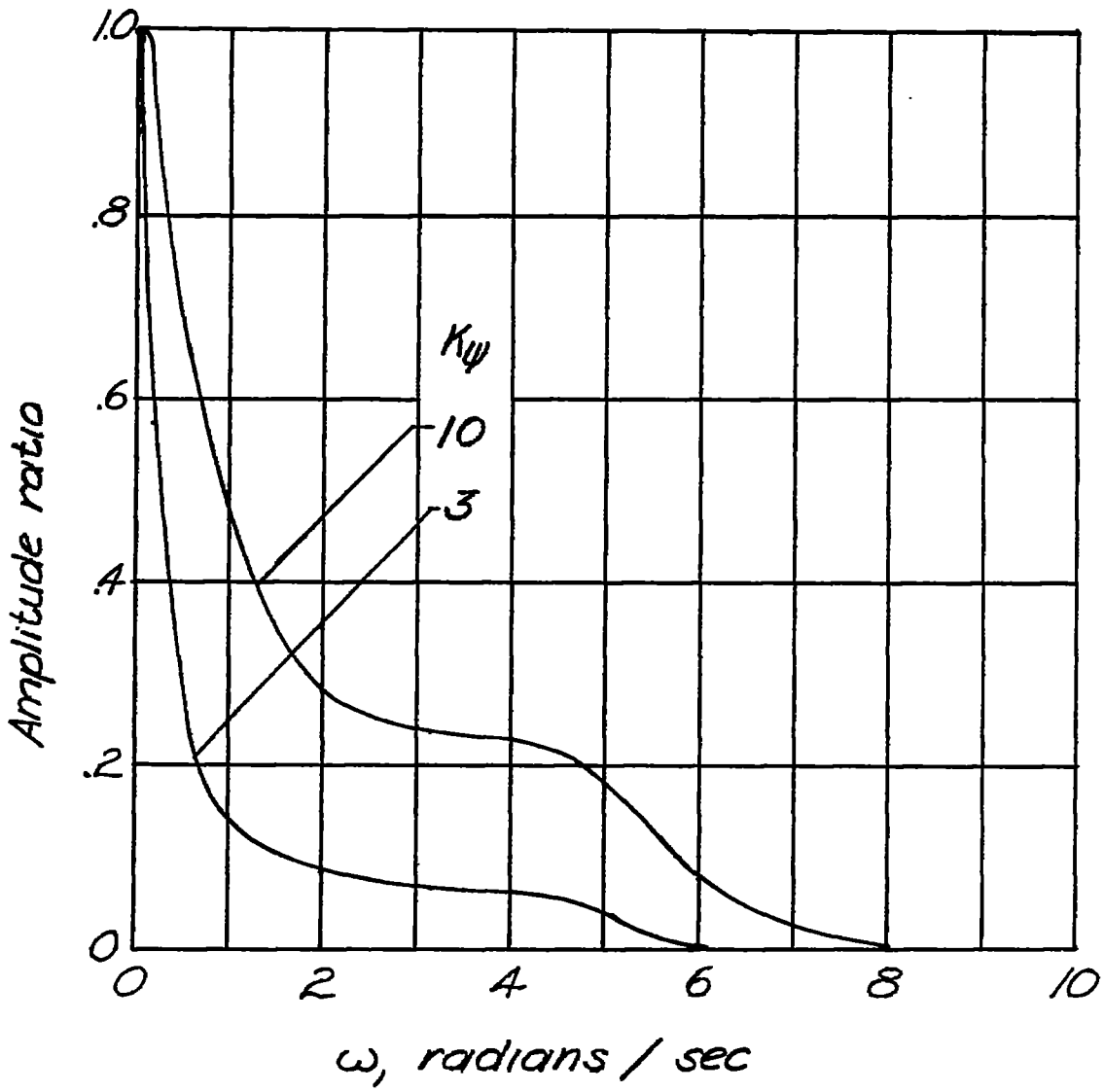

Figure 11.- Frequency response in heading to heading commands for the airplane-autopilot system for two different gain settings of the autopilot heading signal.